

UNPUBLISHED PRELIMINARY DATA

THE THERMAL DECOMPOSITION OF CLCN

by

David Schofield, Wing Tsang and S. H. Bauer

Department of Chemistry

Cornell University

Ithaca, New York

GPO PRICE \$

OTS PRICE(S) \$

Hard copy (HC) 2.00

Microfiche (MF) .50

N65 17062
(ACCESSION NUMBER)
31
(PAGES)
CR 50672
(NASA CR OR TMX OR AD NUMBER)

(THRU)

(CODE)

(CATEGORY)

ABSTRACT

The thermal decomposition of cyanogen chloride was studied in a shock tube, using specific absorption spectroscopy to follow the concentration of CN radicals as a function of time behind the shock wave. This investigation is similar to the previously studied dissociation of cyanogen, but the kinetics are much more complex because of the possibility of reactions involving the unlike radicals CN and Cl.

A mechanism involving six reactions is proposed; these account for all features characterizing the observed results. Values for some ratios of rate constants have been obtained by direct analysis of the CN absorption curves. A method of trial curve fitting using a digital computer was used to deduce the absolute values of the rate constants for the important steps.

CR-50,672

INTRODUCTION

The heat of formation of CN is still subject to debate. Among the recent reports on this quantity, two shock tube studies gave 109 and 99 kcal/mole^{1,2}; mass spectrometric investigations of cyanogen, cyanogen halides and cyanoacetylenes led to 89 kcal/mole³, while a mass spectrometric analysis of the vapor in equilibrium with nitrogen and graphite at elevated temperatures gave 109 kcal/mole⁴. Of equal interest are the rates and activation energies of dissociation of C₂N₂ and XCN (X = halogens, -C₂H). In general, similarities between the characteristic features of the dissociation of the halogen diatoms and these compounds are to be anticipated⁵; the CN group behaves as a rigid unit but it possesses more degrees of freedom than does a mass point. Also at sufficiently high temperatures, the two CN's react to produce N₂ + C₂. A shock tube study of the pyrolysis of BrCN, in the temperature range 2500 - 7000°K has been reported⁶; the kinetics was followed from the emission of characteristic radiation by CN and C₂.

This is a preliminary report on a shock tube study of the dissociation of ClCN over the temperature range 2000 - 2800°K, as followed by absorption at (0,0) band head of the $B^2 \Sigma^+ \longrightarrow X^2 \Sigma^+$ of CN ($\lambda 3883$), using the technique developed for the study of the C₂N₂ dissociation¹. Attempts were made to obtain both the ΔH_{diss}^0 from equilibrium conditions far behind the shock front, and the kinetics of the process from the shock front structure. In the former, we have not yet succeeded. The latter proved much more complicated than the analogous dissociation of C₂N₂

because of the relatively large number of reactions in which the products of the initial dissociation can participate.

EXPERIMENTAL

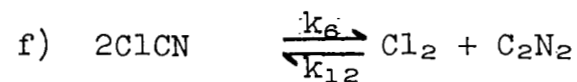
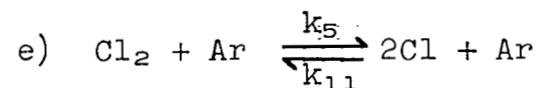
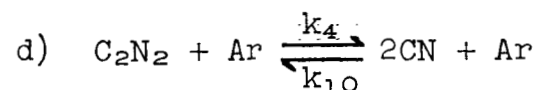
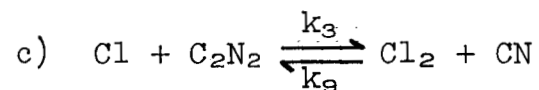
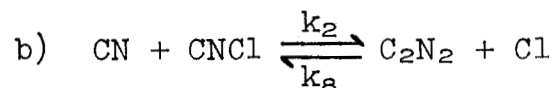
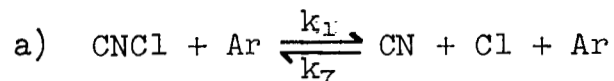
Cyanide chloride was obtained from the American Cyanamid Co. It was condensed at -78°C (dry ice/acetone) and pumped-on to remove volatile impurities. 5% and 0.5% mixtures were prepared with Matheson 99.998% argon, in 12 litre bulbs. These were allowed to stand overnight before use. Mass spectrometric analysis showed that the small water peak initially present was removed by passing the argon through P_2O_5 before mixing.

The shock tube and associated equipment are shown schematically in Fig. 1. The tube was brass, 1 1/2" I.D.; scribed brass diaphragms were used. The concentration of the CN radical behind the shock was followed by means of specific absorption spectroscopy. Details of this method, and of the tube itself, have been given in our reports⁷. The source was a flash tube containing 10mm butane, 3mm nitrogen and 15mm argon. With 200 Ω resistance and sufficient inductance in series with the condenser bank, the emitted CN radiation pulse was substantially flat for 500-600 μs . For nearly all this work the absorption intensity was measured at the (0 - 0) ($3883\overset{\text{O}}{\text{\AA}}$) band of the B, $^2\Sigma^+ \longrightarrow \text{X}, ^2\Sigma^+$ (ground state) of CN. A Jarrell-Ash 8200 monochrometer with 25 μ entrance and exit slits was set for maximum signal from the flash tube. This corresponds to a bandwidth of $0.75\overset{\text{O}}{\text{\AA}}$ at the head of the P branch and encompasses the line from about $J \neq 20$ to $J = 37$. Incident

shocks were run to produce temperatures in the range 2000 - 2800°K. In addition to the CNCl/argon mixtures, some shocks were run with CNCl/Cl₂/argon mixtures, with CNCl:Cl₂ = 3:1. Further experimental details are summarized in Table I.

PROPOSED MECHANISM

The characteristic form of the curve for CN concentration as a function of time behind the shock is a fast initial rise, a flatter portion, and a final rise to the equilibrium value. This is shown in Fig. 2, Curve B. Under various conditions the initial region becomes too short (A) or too small (C) to be observed. To account for these curves the following six reactions, with their inverses, are postulated:



The fast initial rise corresponds to the rapid production of CN in (a). This CN is used up in (b), which is very fast, so that a quasi-steady state is reached. As more of the CNCl

becomes converted to C_2N_2 , (d) becomes important and (CN) finally^{4.} rises to its equilibrium value.

The rate equations for the system are

$$\begin{aligned} \frac{d(CN)}{dt} = & K_1(Ar)(CNCl) - K_2(CN)(CNCl) + K_3(Cl)(CNCl) + 2K_4(C_2N_2)(Ar) \\ & - K_7(Ar)(CN)(Cl) + K_8(Cl)(C_2N_2) - K_9(CN)(Cl) - 2K_{10}(Ar)(CN)^2 \end{aligned}$$

$$\begin{aligned} \frac{d(Cl)}{dt} = & K_1(Ar)(CNCl) + K_2(CN)(CNCl) - K_3(Cl)(CNCl) + 2K_5(Cl_2)(Ar) \\ & - K_7(Ar)(CN)(Cl) - K_8(Cl)(C_2N_2) + K_9(CN)(Cl_2) - 2K_{11}(Ar)(Cl)^2 \end{aligned}$$

$$\begin{aligned} \frac{d(CNCl)}{dt} = & - K_1(Ar)(CNCl) - K_2(CN)(CNCl) - K_3(Cl)(CNCl) - 2K_6(CNCl)^2 \\ & + K_7(Ar)(CN)(Cl) + K_8(Cl)(C_2N_2) + K_9(CN)(Cl_2) + 2K_{12}(C_2N_2)(Cl_2) \end{aligned}$$

In the case where only CNCl and argon are present initially, the concentrations are related by

$$\begin{aligned} (CNCl)_{t=0} &= (CNCl) + (CN) + 2(C_2N_2) \\ &= (CNCl) + (Cl) + 2(Cl_2) \end{aligned}$$

These expressions can be simplified. Call $(CNCl)_{t=0} \equiv \phi$, and express all the concentrations relative to ϕ :

$$\begin{aligned} x &= (CNCl) / \phi \\ y &= (CN) / \phi \\ z &= (Cl) / \phi \\ p &= (C_2N_2) / \phi &= 1 - x - y \\ q &= (Cl_2) / \phi &= 1 - x - z \end{aligned}$$

Then

$$\begin{aligned} \frac{dx}{dt} = & -C_1x - C_2xy - C_3xz - C_6x^2 \\ & + C_7yz + C_8pz + C_9gz + C_{12}pq \end{aligned} \quad (1)$$

$$\begin{aligned} \frac{dy}{dt} = & C_1x - C_2xy + C_3xz + C_4p \\ & - C_7yz + C_8pz - C_9gz - C_{10}y^2 \end{aligned} \quad (2)$$

$$\begin{aligned} \frac{dz}{dt} = & C_1x + C_2xy - C_3xz + C_5g \\ & - C_7yz - C_8pz + C_9gy - C_{11}z^2 \end{aligned} \quad (3)$$

where

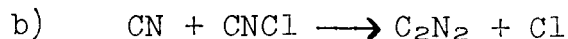
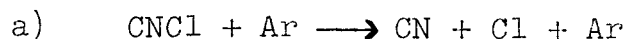
$$\begin{aligned} C_1 &= K_1(\text{Ar}) & C_7 &= K_7(\text{Ar}) \phi \\ C_2 &= K_2 \phi & C_8 &= K_8 \phi \\ C_3 &= K_3 \phi & C_9 &= K_9 \phi \\ C_4 &= 2K_4(\text{Ar}) & C_{10} &= 2K_{10} \phi (\text{Ar}) \\ C_5 &= 2K_5(\text{Ar}) & C_{11} &= 2K_{11} \phi (\text{Ar}) \\ C_6 &= 2K_6 \phi & C_{12} &= 2K_{12} \phi \end{aligned}$$

At $t = 0$, $x = 1$ and all the other concentrations (except (AR)) are zero. These equations were programmed for solution on a Burroughs No. 220 digital computer using the Runge-Kutta method. Initial time intervals of $1 \mu\text{s}$ were used; this was found to be adequate for the first $10 \mu\text{sec}$. The interval was increased progressively, the later values being found individually by solving in decreasing steps: typically $20 \mu\text{s}$.

APPROXIMATE SOLUTIONS FOR SHORT TIMES

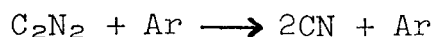
For the initial period there is an approximate analytic solution. Taking reactions (a) and (b) alone, and neglecting the de-

pletion of CNCl



$$\text{Then} \quad (\text{CN}) = (\text{Ar}) \frac{K_1}{K_2} (1 - e^{-K_2 t}) \quad (4)$$

This shows how the CN reaches a steady state concentration of $K_1(\text{Ar}) / K_2$. (Fig. 3a). In the next approximation include also reaction (d):



(b) is so rapid that, except during the initial fast rise, nearly all the CN formed in (a) ends up as C_2N_2 . Thus, neglecting CNCl depletion, $(\text{C}_2\text{N}_2) \approx K_1(\text{Ar}) t$. This will overestimate (C_2N_2) when t is small, but (C_2N_2) is itself small under these conditions. Hence (Fig. 3b)

$$(\text{CN}) = \frac{K_1(\text{Ar})}{K_2} \left[1 + \frac{2K_4(\text{Ar})}{K_2} (K_2 t - 1) - \left(1 - \frac{2K_4(\text{Ar})}{K_2} \right) e^{-K_2 t} \right] \quad (5)$$

Comparison with machine calculations shows that this is a good approximation for the initial period (Fig. 4), assuming the mechanism proposed above.

From the above expression three quantities may be extracted, based on the initial portion of the experimental curve, (see Fig. 3b):

- 1) The time at which the linear term starts to dominate the exponential term in (5). This occurs when $t \approx 3/K_2 = \tau$

- ii) the value of (CN) at $t = 0$, obtained by projecting backwards the linear portion of the curve. Call this A.
- iii) the slope of the linear portion. Call this B. From (5) we see that

$$A = \frac{K_1(\text{Ar})}{K_2} - \frac{2K_1K_4(\text{Ar})^2}{K_2\phi} \quad (6)$$

$$B = \frac{K_1K_4(\text{Ar})^2}{K_2} \quad (7)$$

THERMOCHEMISTRY

In order to relate the observed shock velocity to temperature and composition of the gas, it is necessary to know the enthalpies of the species present. The values used are summarized in Table II. The species considered are

Ar	CNCl	CN	Cl	C ₂ N ₂	Cl ₂	C ₂	N ₂
----	------	----	----	-------------------------------	-----------------	----------------	----------------

Shock temperatures were calculated for the case of no reaction, and for various equilibrium conditions involving some or all of the above species. The equilibrium constants were formed from the free energies, and are listed in Table III. All the thermochemical quantities were obtained from JANAF thermochemical tables except the heat of formation of CN. As some doubt exists as to the value of this quantity, five values ranging from 91.2 to 109.4 kcal/mole were used. All the kinetic analyses are based on the value 99.4, which make the dissociation energy of cyanogen 125 kcal/mole¹. The similar analyses based on the other four values have yet to be completed.

ABSORPTION COEFFICIENT OF CN

The absorption coefficient for CN was found by comparing the observed absorption, when the CN had reached equilibrium, with the calculated equilibrium concentration appropriate to the observed shock velocity. In these equilibria the species considered were:



The CN absorption remained flat after equilibrium was reached. The results (Fig.5) are rather scattered, because the absorption is large, and a small error on the oscilloscope trace introduces a large error in the absorption coefficient. It was not possible to reduce either the density or temperature, because the testing time (400 μ s) would have been too short to permit the attainment of equilibrium. Most of the points are for 5% CNCl/argon, for this reason, though most of the kinetic analysis is based on 1/2% CNCl/argon.

Emission from the shocked gas was negligible compared with that from the source (this was shown experimentally). Hence

$$(\text{CN}) = x \ln(I_0/I) \quad (8)$$

with $x = 2.27 \times 10^{-6}$, when (CN) is measured in moles/litre. This is about twice the value found previously (1), from the dissociation of C_2N_2 , using a similar set-up (1.15×10^{-6}).

ANALYSIS OF DATA

Initial Period:

The experimental curves give the transmitted intensity ratio vs time, in laboratory coordinates. One must then deduce the

quantities A,B [see Fig. (3b) and eqs.(6),(7)] from these curves.^{9.}

If the total absorption is small, so that [cf: Eq.(8)]

$$(I_0 - I) \approx x I_0 (CN) = x I_0 y \phi \quad (9)$$

intercepts and slopes (A' and B') may directly be estimated from the oscilloscope traces (Fig. 6).

$$A' = A \times I_0 \quad (10)$$

$$B' = B \times I_0 \cdot \frac{\rho_2}{\rho_1} \quad (11)$$

where the factor (xI_0) converts (CN) to I, and the density ratio

$\frac{\rho_2}{\rho_1}$ converts t_{LAB} to the kinetic (particle flow) time. On

neglecting the second term in (6),

$$A \approx \frac{k_1(Ar)}{k_2}$$

Fig.(7) shows a plot of $\log \left(\frac{A}{\phi} \right)$ vs $\frac{1}{T}$ for some 1/2% CNCl shocks for which $A/\phi \approx 200 K_1/K_2$. In theory K_2 can be found from the time taken for a quasi-steady-state concentration to appear. However, these results show a large scatter, (Fig. 8), as they are based on a very small portion of the oscilloscope trace.

The activation energy of reaction (b) must be low (cf. Table II). A value of 6 kcal was selected and a line drawn through the points of Fig. 8. With this value for K_2 , and the above approximation for (K_1/K_2) , the values of B can be used to derive K_4 . The points are shown on Fig. 9. Finally, from K_4 and K_2 , K_1 may be

calculated based on the experimental values of A, on the basis of the exact formula (6). The points are shown in Fig. 10. These results are more consistent than are the points plotted in Fig. 7 because of the inclusion of the second term in Eq. (6).

Curve Fitting:

The above procedure gave suitable initial trial values for K_1 , K_2 and K_4 . Then K_3 , K_5 and K_6 were estimated and trial calculations run on a digital computer. The rate constants were assumed to have the form $Ae^{-E/RT}$, with magnitudes for the parameters indicated as 'First Trial', listed in Table IV. The calculated curves (a) are shown, superimposed on the experimental results, in Figs. 11, 12. On the whole they rise too rapidly. Hence, a second trial fit was made (b) with a reduced value for the pre-exponential factor of K_4 (cyanogen dissociation rate).

A third set of curves computed with slightly adjusted values, is shown in Figs. 13 - 15. Increasing K_3 makes the slow-rising curves faster without altering the rapid ones. However, the curves are fairly insensitive to variations in K_3 . Reaction (f) is too slow to be important.

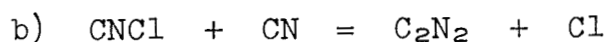
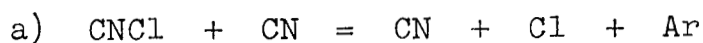
The dissociation of chlorine, reaction (e), is certainly faster than the K_5 used. However, the main supply of Cl atoms is reaction (b), and the equilibrium lies well over to dissociated side; the process $\text{Cl}_2 \longrightarrow 2\text{Cl}$ is not significant in the mechanism. Introducing a much larger K_5 , would require that

the integration be performed with much smaller steps.

Several curve fits for 5% CNCl/Ar mixtures are given in Fig. 16. For this concentration there is a larger temperature change caused by the reaction. Kinetic curves are shown computed for the 'no-reaction' and the 'equilibrium' temperatures. The former give much better fits, as would be expected.

CONCLUSIONS

Although the reaction is too complex to analyze completely, the mechanism given, together with reasonable rate constants, is capable of representing the shape and variation of the observed cyanogen concentration with time. The ratio of rates (a) and (b)



has been found directly to be

$$\frac{K_1}{K_2} = 3.1 \times 10^3 e^{-85,500/RT}$$

K_2 has been placed as to its order of magnitude (Fig. 8). The best fits for the observed curve were computed with a value for the dissociation rate constant for C_2N_2 of $10^{14.23} e^{-100,400/RT}$ litres/mole sec which is almost identical with that reported previously¹. These rates lead indirectly to a value for $(\text{CNCl} + \text{Ar} \longrightarrow \text{CN} + \text{Cl} + \text{Ar})$ of $K_1 = 10^{13.53} e^{-91,500/RT}$ litres/mole sec.

ACKNOWLEDGEMENT

This work was supported by a grant from NASA (NsG-116-61), to whom grateful acknowledgement is made.

REFERENCES

1. W. Tsang, S. H. Bauer and M. Cowperthwaite, J. Chem. Phys., 36, 1768 (1962)
2. H. T. Knight and J. P. Rink, J. Chem. Phys., 35, 199 (1961)
3. V. H. Dibeler, R. M. Reese and J. L. Franklin, J. Amer. Chem. Soc., 83, 1813 (1961)
4. J. Berkowitz, J. Chem. Phys., 36, 2533 (1962)
5. For recent papers on this topic refer to the 33rd Discussion of the Faraday Society (1962). cf. contributions by J.C. Kick (p.182) and G. Porter (p.198). Also:
H. Hiraoka and R. Hardwick, J. Chem. Phys., 36, 1715 (1962)
6. W. L. Patterson and E. F. Greene, J. Chem. Phys., 36, 1146 (1962)
7. S. H. Bauer, et al: Technical Report to the Air Force
Aeronautical Research Laboratory, Office of Aerospace Research USAF, ARL-100, December, 1961.

TABLE II

ΔH° for reactions a-f at 2000°K and 2800°K kcal/mole,
assuming $\Delta H^\circ_{\text{form}}(\text{CN}) = 99.4$

	(a)	(b)	(c)	(d)	(e)	(f)
ΔH°_{2000}	96.73	-26.42	36.15	123.15	60.58	9.73
ΔH°_{2800}	96.64	-25.39	35.32	122.03	61.32	9.93

TABLE III

EQUILIBRIUM CONSTS. K_c FOR REACTIONS a-fassuming $\Delta H_f(\text{CN}) = 99.4$ kcal/mole

units: moles/litre

T °K	$\log_{10} K_c$ (a)	(b)	(c)	(d)	(e)	(f)
2000	-5.847	1.969	-3.375	-7.816	-2.471	-1.406
2200	-4.930	1.709	-3.020	-6.640	-1.911	-1.311
2400	-3.834	1.400	-2.593	-5.234	-1.240	-1.193
2600	-2.978	1.160	-2.262	-4.138	-0.716	-1.101

TABLE IV

PARAMETERS USED IN CURVE FITTING

Rate constants are of form: $K = Ae^{-E/RT}$

	curve fit	(i)	(ii)	(iii)	E
$\log_{10} A$	(1)	13.53	13.53	13.53	91.5
"	(2)	10.05	10.05	10.05	6
"	(3)	10	10	11	34
"	(4)	14.61	14.3	14.23	100.4
"	(5)	10	10	10	40.6
"	(6)	10	10	10	60

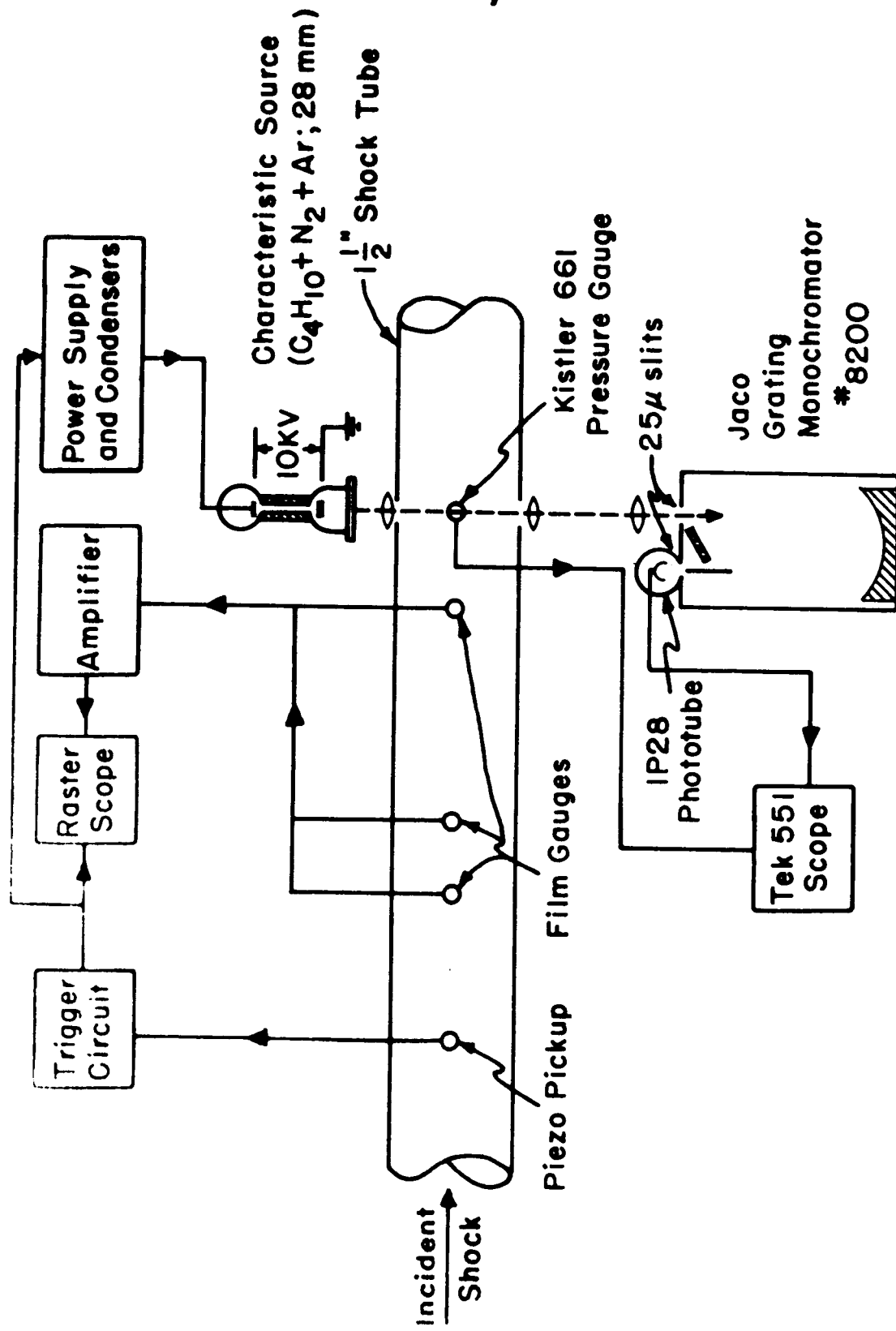


Fig. 1 Block Diagram of Apparatus

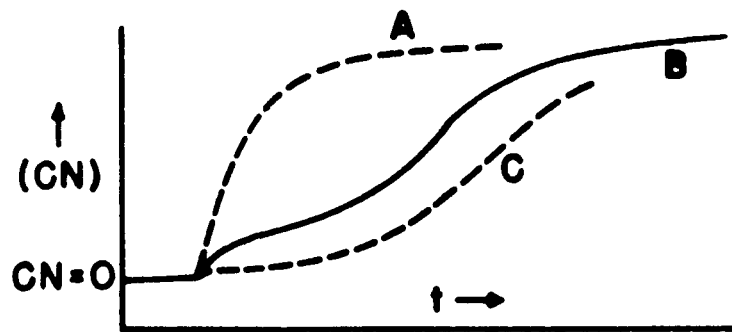
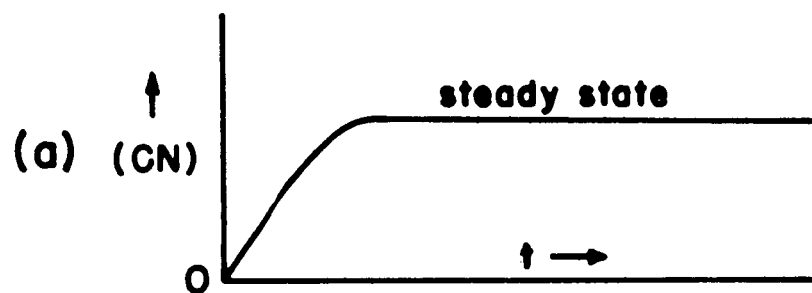
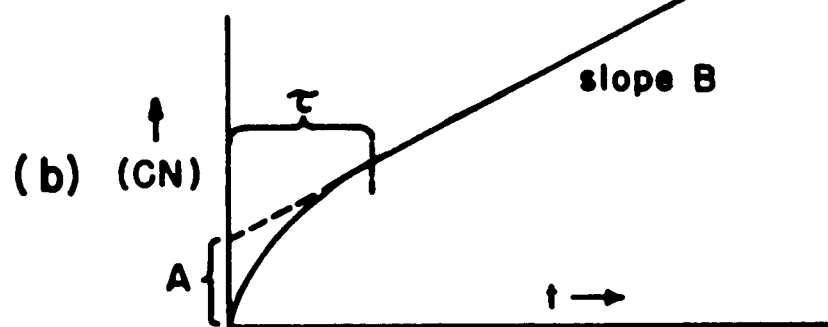


Fig. 2 Typical observed form of CN concentrations behind the shock wave.



Equation (4)



Equation (5)

Fig. 3 Initial Approximations

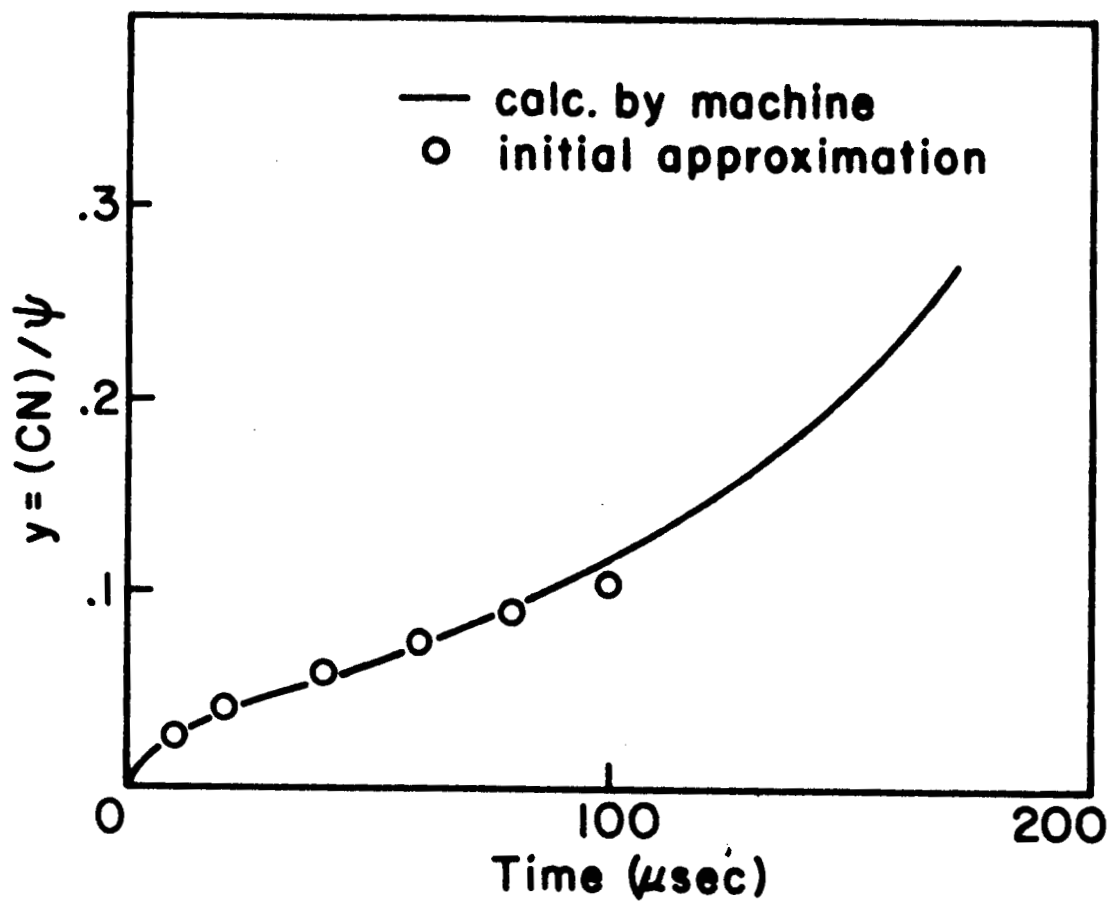


Fig. 4

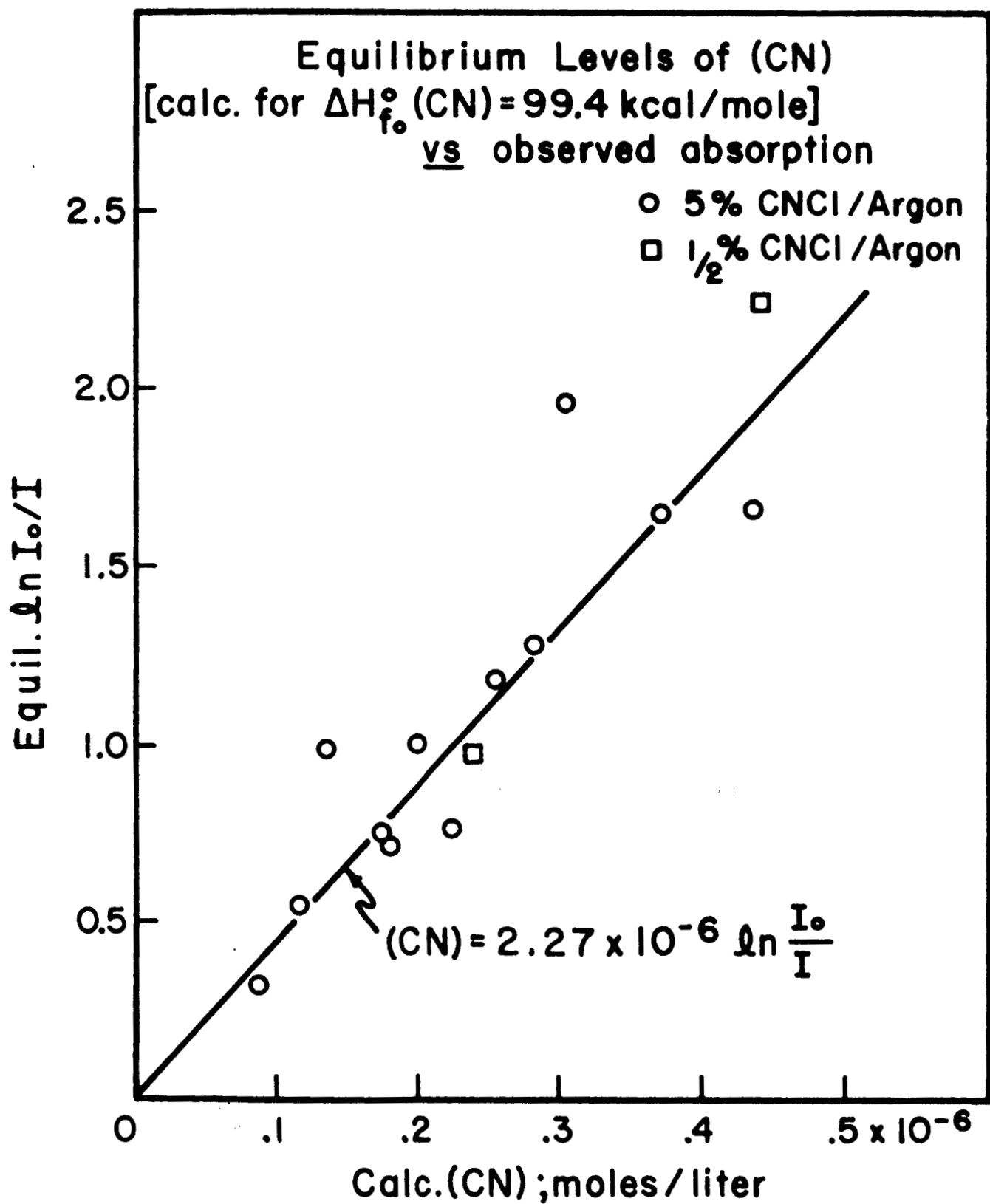


Fig. 5

Key to Absorption Pictures

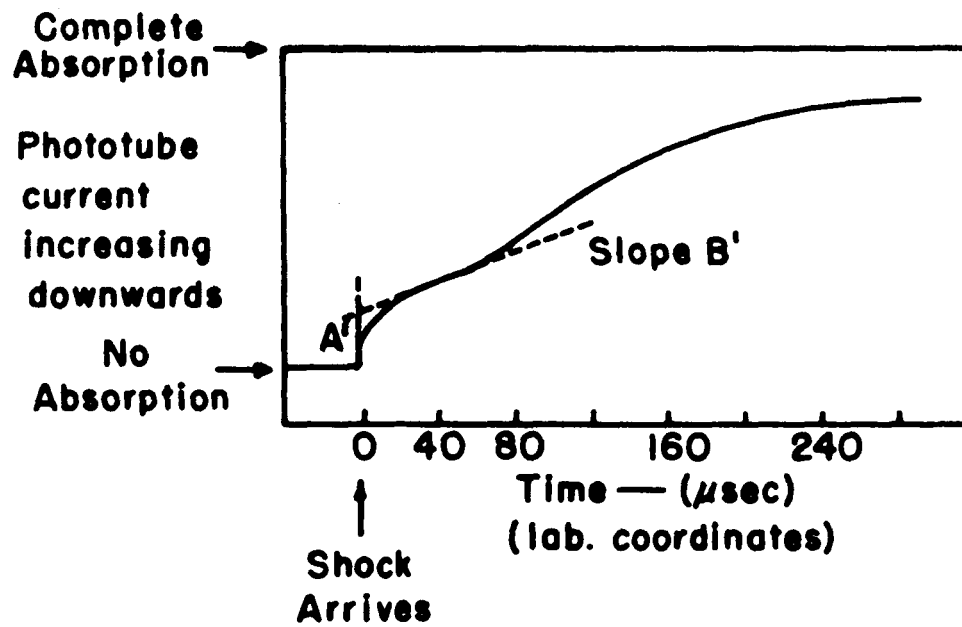


Fig. 6

Analysis of Initial Stages

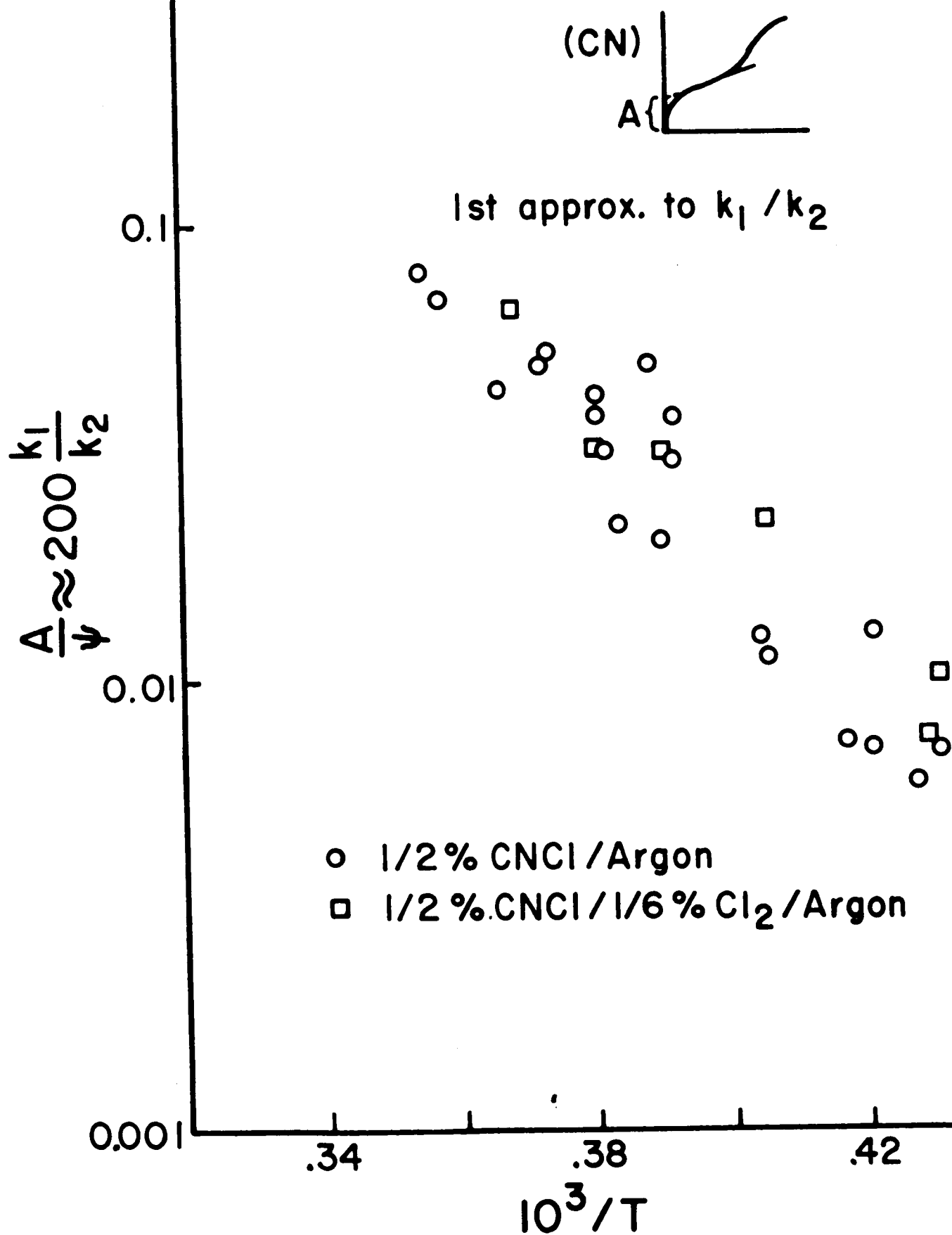
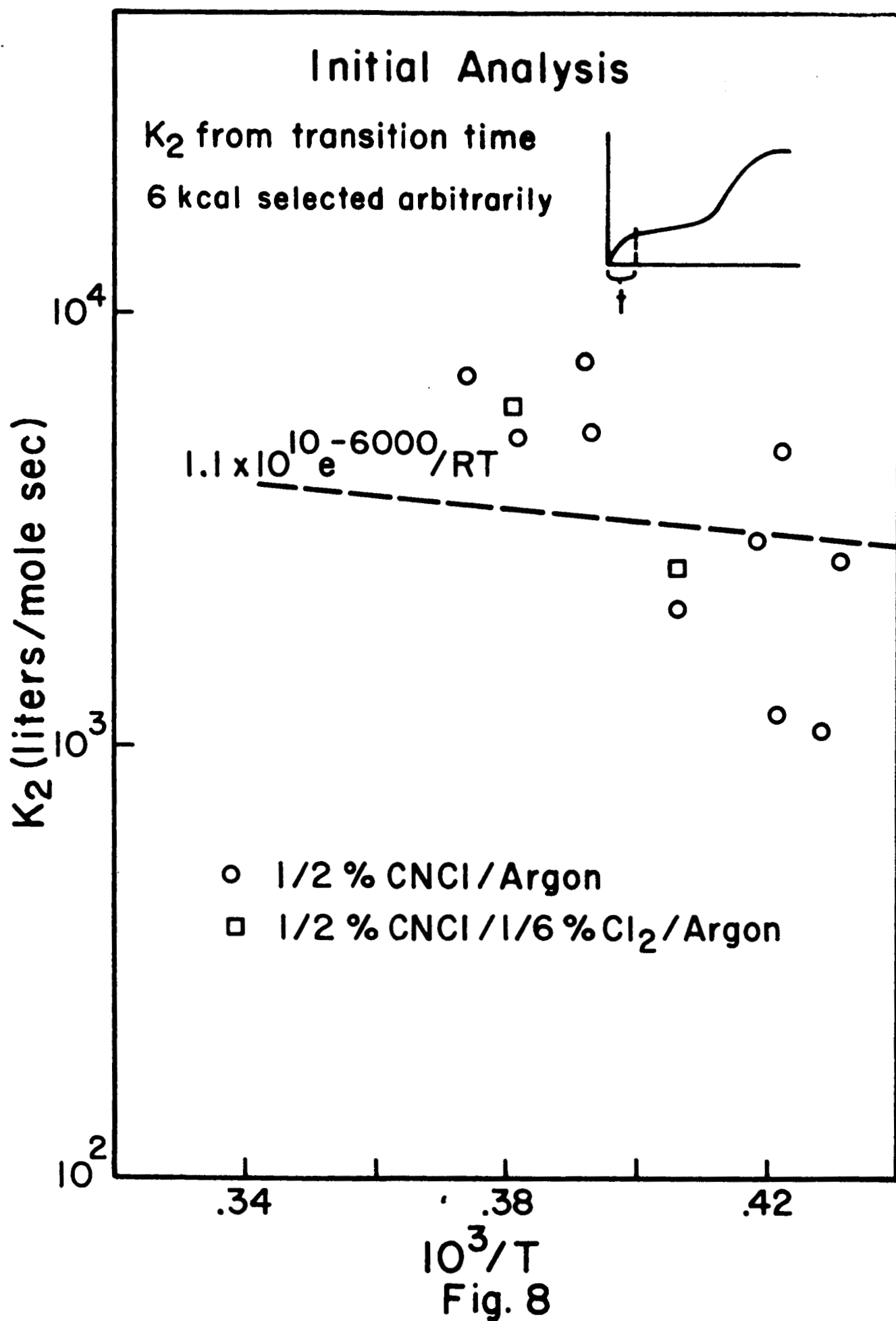


Fig. 7



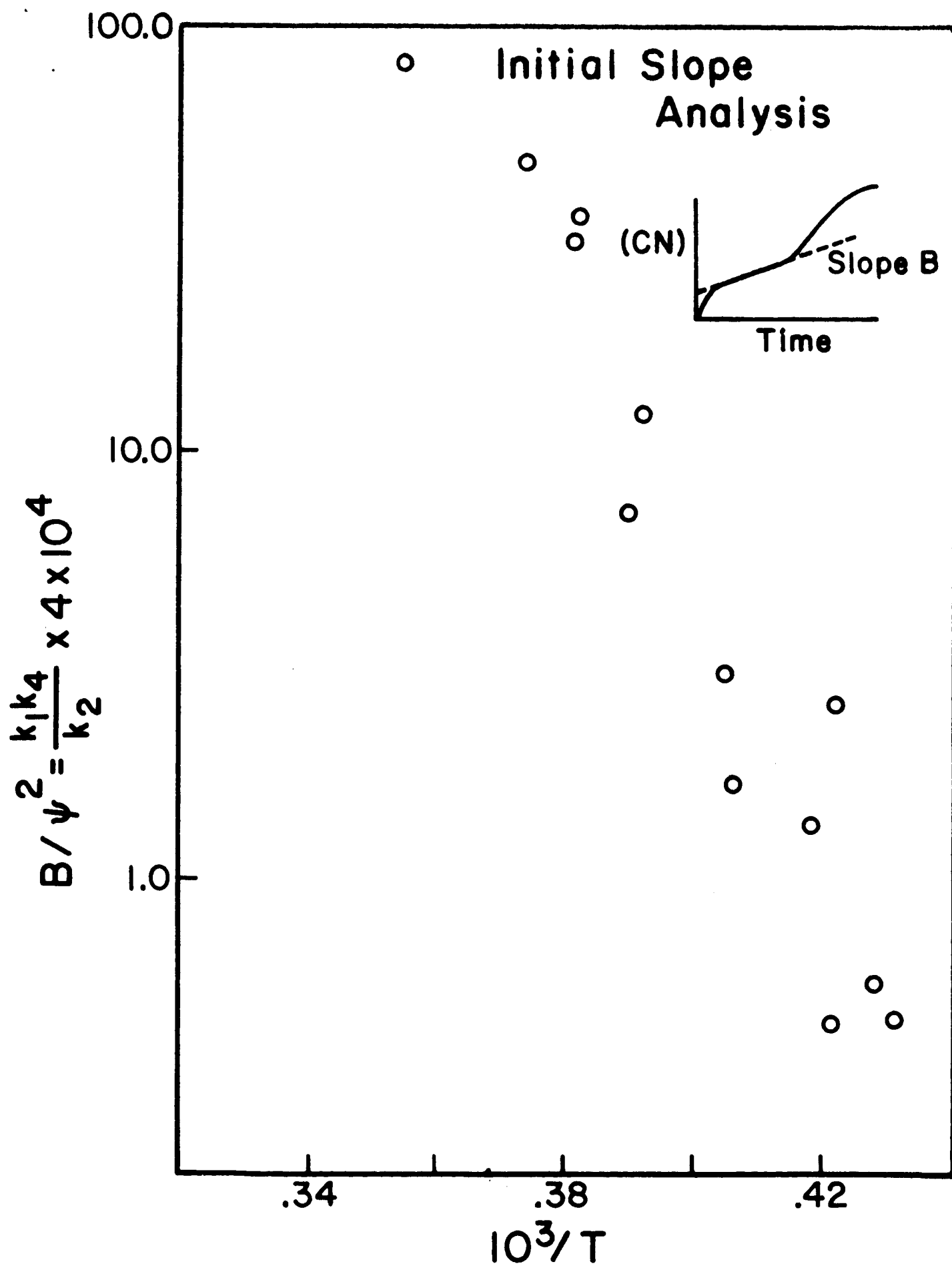


Fig. 9

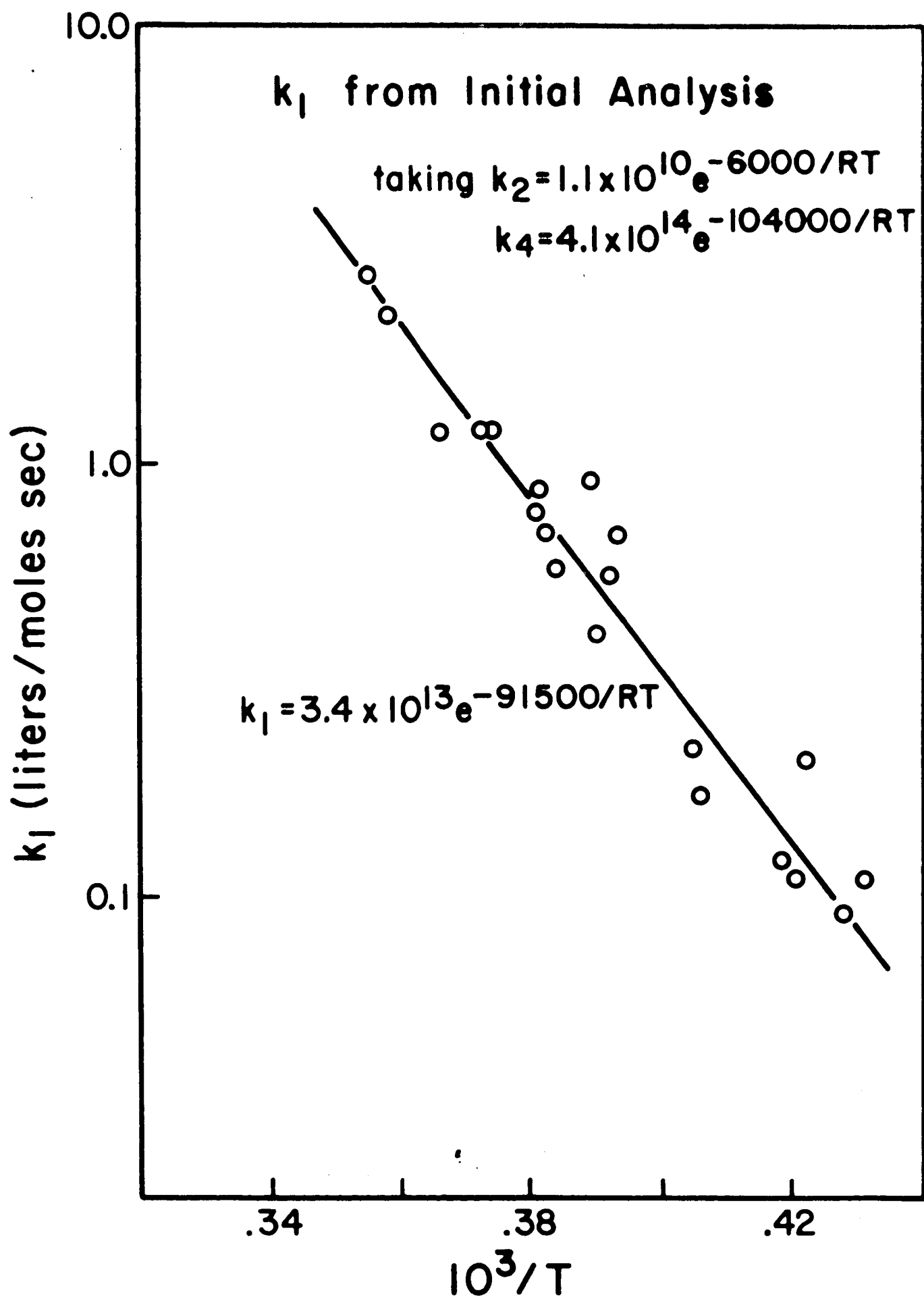
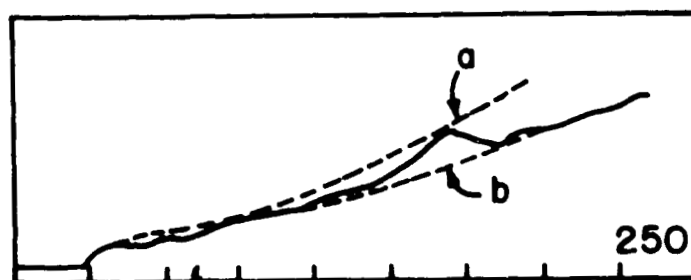
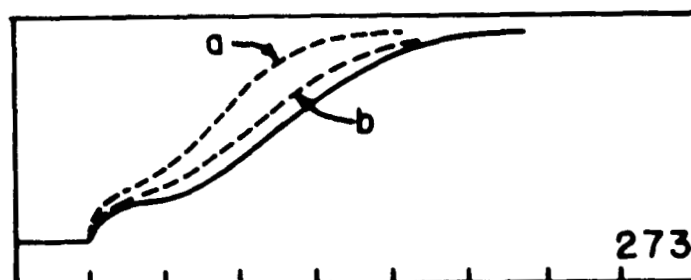
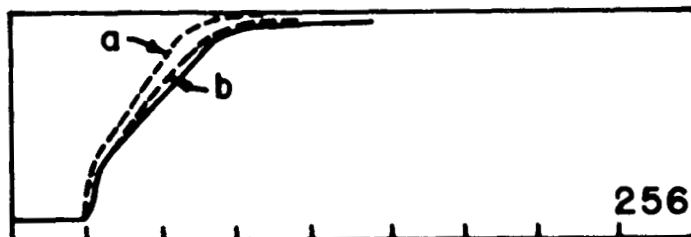
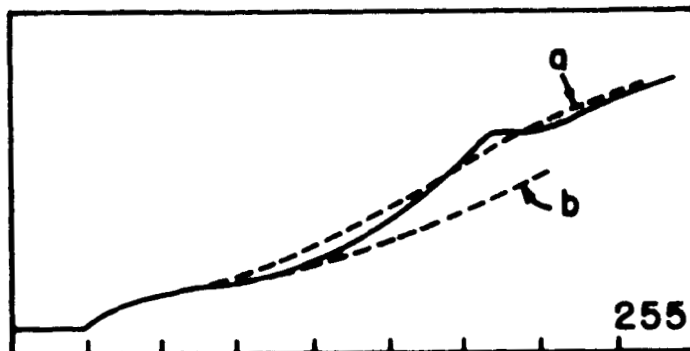


Fig. 10

Curve Fitting

a First trial } — experiment
b Second trial }

See key, Fig. 6



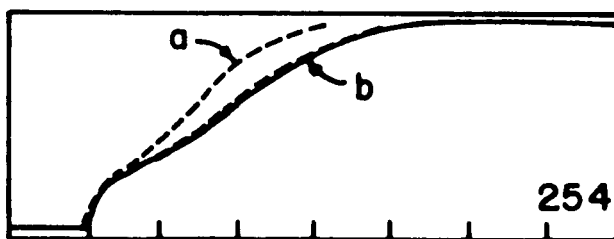
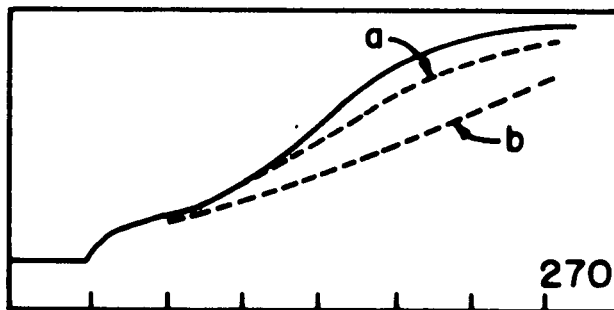
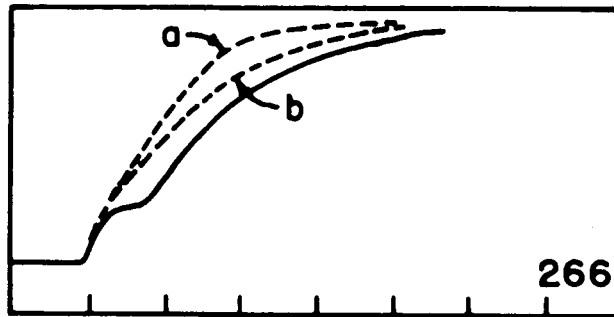
All $40 \mu\text{s}/\text{cm}$

Fig. II

Curve Fitting

a 1st trial

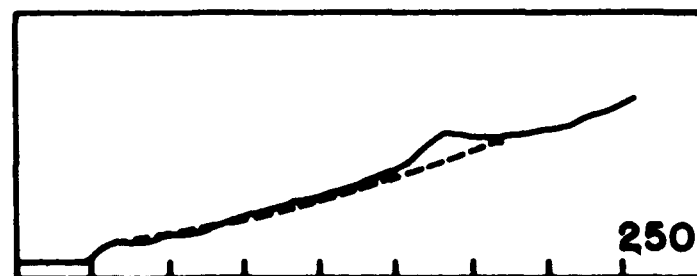
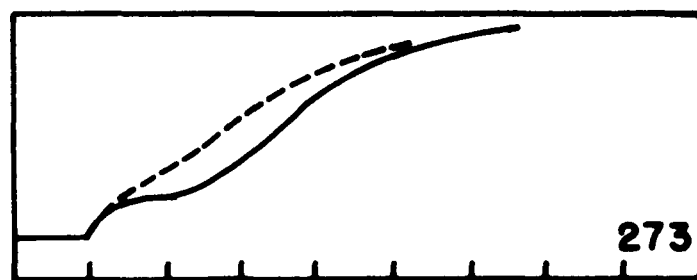
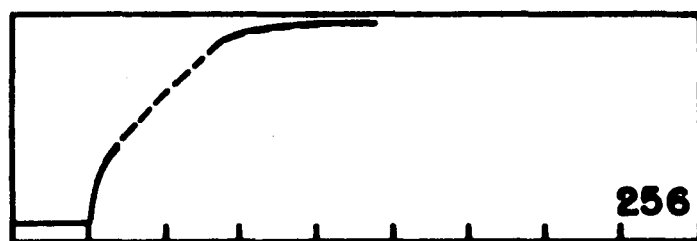
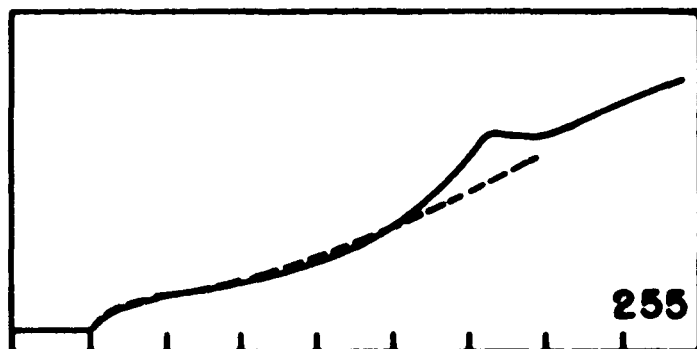
b 2nd trial



All 40 $\mu\text{s}/\text{cm}$

Fig. 12

$\frac{1}{2}\%$ CNCl / Argon
3rd curve fit

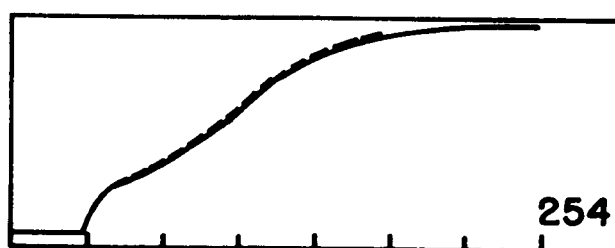
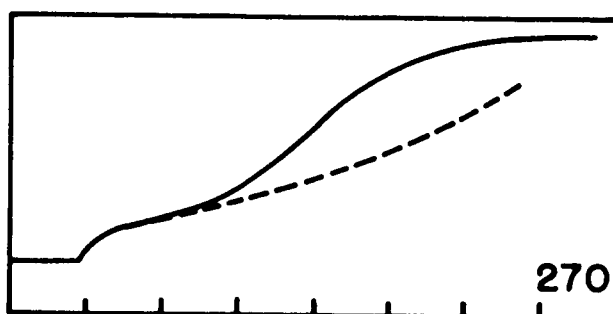
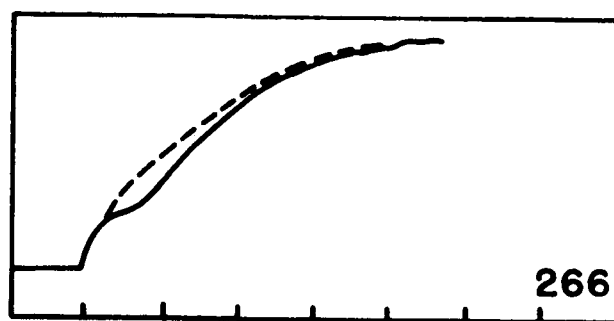


All $40\mu\text{s}/\text{cm}$

----calc.
——exp't

Fig. 13

$\frac{1}{2}$ % CNCl / Argon
3rd curve fit

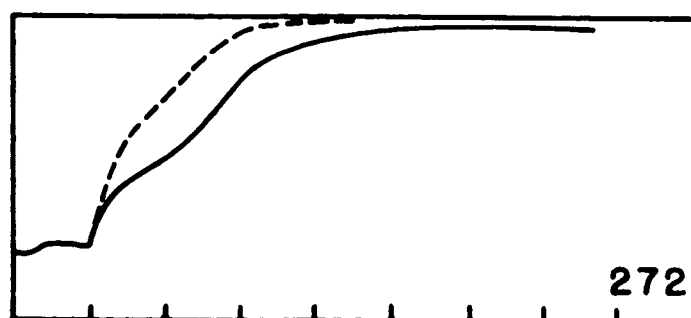
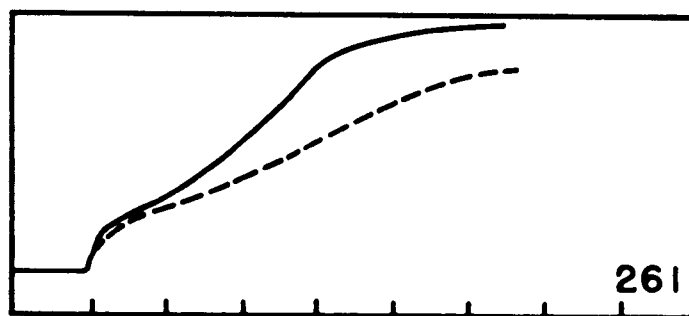
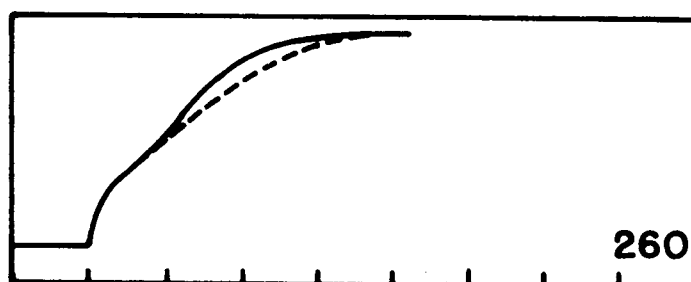
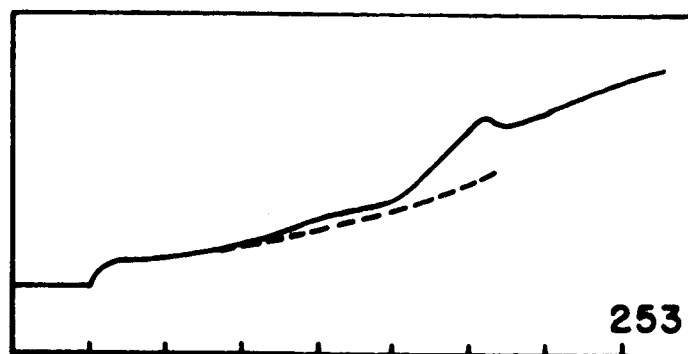


All $40 \mu\text{s}/\text{cm}$

— exp't
--- calc.

Fig. 14

3rd curve fit cont'd



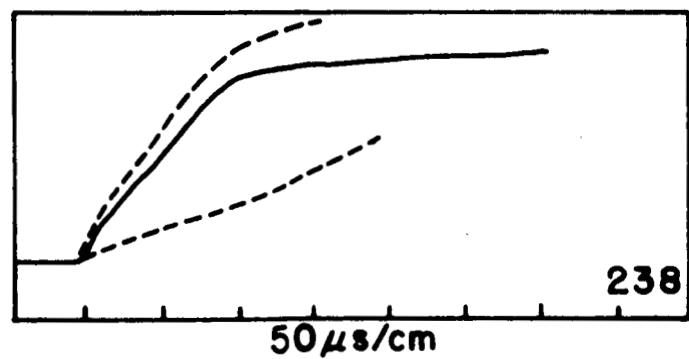
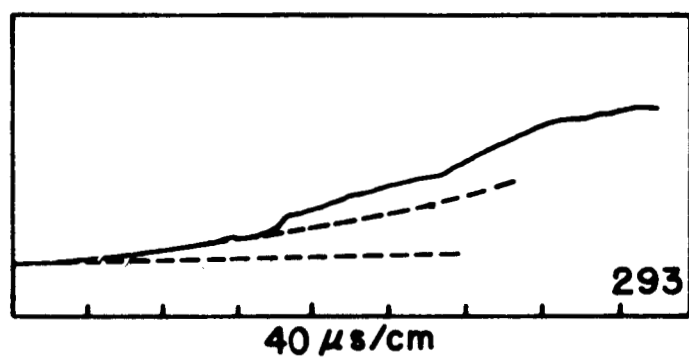
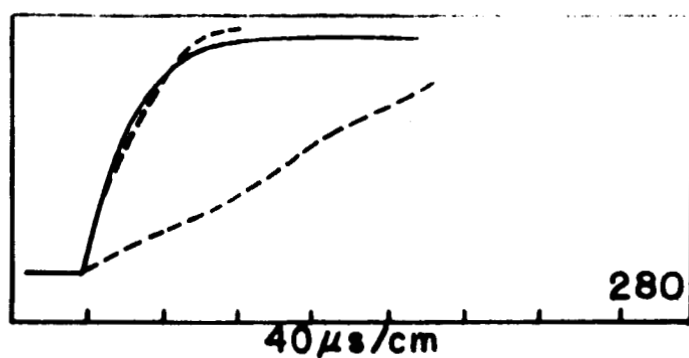
All $40\mu\text{s}/\text{cm}$

--- calc.

— exp't

Fig. 15

5% CNCl/Argon shocks
3rd curve fit



---- upper: calc. for initial temp.
---- lower: calc. for equilibrium temp.
— experimental

Fig. 16